Investigation and Development of a Laminar Foam Trauma Pack For Use With Personal Ballistic Body Armor

Andrew Miles

Mechanical Engineering (BEng) Degree

Matriculation No. 0507347

Final Year Project Report

Department of Mechanial Engineering

University of Glasgow

COMPLETED APRIL 2009

Table of Contents

List of Figures

Introduction

The basis of the project is to investigate the effectiveness of a laminar foam trauma pack to be used with body armour.

When a projectile strikes body armour although it is stopped injury can still be caused by two distinct mechanisms; localised deformation directly behind the armour, due to out-of-plane displacement of the armour into the body and also via a the shock wave created due to the rapid deceleration and transfer of energy from the projectile to the armour which propagates through the body. Injuries due to the shock wave are classified as ‘behind armour blunt trauma’ (BABT) or ‘rear effect’ and can in some cases result in fatality. In this situation the armour distributes the impact energy over a large area, causing global deformation of the chest. Life-threatening rear effects include severe lung and heart contusions as well as rib fractures [1]. The localised deformation of the body armor can cause ‘rear effect signature injury’, lacerations that occur due to blunt trauma. Although the vest is successful in stopping the round it is not effectively dissipating the energy enough to stop large deformation on the back face of the armour in the area of impact. The deformation of the tissue exceeds the threshold of skin and a penetrating wound results. These two different types of injuries can occur together [2].

The back face signature (BFS) of body armour is classed as the distance between the original plane of the back face of the armour and the point of maximum displacement in the direction of the projectile line of flight. National Institute of Justice states that the back face signature for ballistic resistance of personal body armour should be no more than 44mm [3].

The aim of this work is to investigate the most effective way of using polyurethane (PU) foam as an integral part of trauma packs with a view to minimising the BFS of personal body armour and the energy transfer to the wearer.

Literature Review

Blunt impact trauma

Gryth [4] set about investigating weather NJI Standard 0101.004 was a sufficient criterion to follow when personal body armor was exposed to high velocity rounds, through the use of anesthetised pigs. Seven of the eighteen pigs shot at died. It was judged that the allowed back face signature of 44mm in oil-based plasticine is not sufficient protection against high velocity rounds. Other previous works relating to BABT have investigated the reasons for such injuries and its effects on the wearer's body through simulation and experimental work. Drobin et al [5] also used anesthetised pigs wearing body armor (including ceramic plates) this time to assess the physical effects of BABT. Half of the shot animals (4 of 8) had rib fractures and all had a lung contusion. This contusion with the accompanying lung hemorrhage was the most serious gross injury in exposed animals. Roberts et al [6] developed a human torso finite element model (HTFEM) enabling the comparison of different body amours and the relative stresses developed in different places in the model, however the model had not been validated against animals or cadavers and so the true damage to the wearer is not necessarily represented by the model.

Comment [MSOffice1]: Define 'lung contusion in an appendix or glossary

Comment [MSOffice2]: define

Foam

Energy absorbers, which foam fits into are a class of products that generally absorb kinetic mechanical energy by compressing or deflecting at a relatively constant stress over an extended distance, and not rebounding. Springs perform a similar function, but they rebound, hence they are energy storage devices, not energy absorbers. Cellular materials are widely used in many applications due to their excellent thermal, buoyancy and energy absorption properties. It is the energy absorption properties that are of interest in this work. Foam has long been used for the protection of items subjected to both static and dynamic loading from cushions and protective packaging to explosive blast protection. [7]

Comment [MSOffice3]: elastic?

The properties of foams are significantly influenced by cell structure. In particular the anisotropy of many foams results in a large difference between the compressive strengths in the rise direction and that perpendicular to rise [8]. Foams are generally split into three categories, open-cell, closed-cell and bead foams. In open cell foams the structure is made up of cell edges, the cell walls collapse during the foaming process, gas is able to pass freely through the foam. Conversely closed cell foams consist of pockets of gas enclosed by cell walls made up of the base material. Bead foams comprise small balls of foam compressed together to form larger blocks. Open cell and bead foams are structurally opposite, were the edges are in the open cell structure air can pass between the balls of foam in bead foam.

Types of ballistic analysis

There are various methods used to measure the ballistic resistance of materials, this makes it difficult to directly compare results form the range of literature on the subject. Methods frequently used include: the V_{50} ballistic limit, linear regression, depth of penetration, energy/areal density and back face signature.

V_{50} analysis involves determining the projectile velocity at which there is a 50% probability it will pass though the test specimen. As this method is based on averaging the velocity of shots passing through the specimen and those not, in order to achieve accurate results a large number of data points are needed. This method is good for assessing the maximum amount of damage an impact threat may incur. [9]

Siriman [7], discussed depth of penetration as an analysis tool. "*When impacting armor, characteristics of the penetration cavity are observed to gain insight into the materials impact absorption mechanisms. This method is also useful when comparing several materials to be used in applications where penetration resistance is required*."

The energy per unit areal density is a useful tool when comparing the ballistic impact resistance of a range of different materials. This method takes into account the specimen dimensions, density and energy of the projectile and has been used in previous work on all polypropylene self-reinforced composites (rsPP). [10]

The Back face signature is classed as "*the greatest extent of indentation in the backing material caused by a non perforating impact on the armor*". The BFS is the perpendicular distance between original plane of the front of the backing material and the deepest point of indentation parallel to it [3]. This is the method to be used in this work, as it is the BFS that cause the blunt impact trauma the trauma pack is intended to reduce.

Laminate foam structures

Sriram [7] states "*sandwich composites have high strength and stiffness compared to monolithic solid plates.*" And looked specifically at the blast impact response of aluminum foam sandwich composites, showing the plastic deformation of aluminum foam consumes kinetic energy which eventually halts the progression of the shock wave produced by the blast. He discusses how foam can be exploited as an energy absorber by mounting a heavy buffer plate in front of it. Shim [11] investigated the static and dynamic response of layered polyurethane foam separated by steel plates, in various geometries. It was shown that the response of a layered system of uniform width under quasi static loading was similarly to an un-layered system of the same geometry and volume of foam. His studies demonstrated the inadequacy of relying on static data and analysis in the examination of dynamic response.

Polyurethane foam characterisation

Specimens

Two types of specimen were made up using CFS Fibreglass Supplies 2 part polyurethane foam liquid (2kg pack), foam blocks and foamed layers. For the foam blocks the two liquid components were mixed (50:50) in a mould, 3.5 ml of each, measured using 10ml syringes, giving block specimens of dimensions 50x50x25mm ± 1mm. Separate syringes were used for each of the two liquids. When the polyurethane expands and rises in the mould it forms a dome shape on the top surface due to the friction between the mould and foam, inhibiting the foams expansion around the edges. In light of this enough of the two part liquid was used to ensure the foam rose over the sides of the mould enabling the dome to be cut off level with the top of the mould leaving specimens of the right height, with parallel top and bottom surfaces. Eight block specimens were made. Despite best efforts to make the specimens identical when the densities were measured a range of results could be seen, see table 1. This was expected because the formation of cells in foam during fabrication occurs via a chemical process, which has a degree of variability.

** Photo of specimen.*

Specimen	1	2	3	4	5	6	7	8	Average
Density	56.10	42.50	45.20	38.30	34.00	42.90	49.70	46.90	44.45

***Table 1**, showing densities of polyurethane foam mixed with one syringe.*

Initial investigations showed that thin sheets of foam could be produced foaming it between two stiff metal plates covered in aluminium foil, to prevent the foam sticking to the plates. Parts A and B were mixed together on one of the plates, spacers were placed between the plates (2mm thick), the second plate was then placed on top and weighted down to prevent the foam rising vertically. The mixture was then left to foam and set.

As large amounts of foam in thin sheets are required the above procedure was up scaled. Large sheets of PU foam were produced in varying thicknesses by using two tables as a press. The tables were covered in cling film in order to stop the foam sticking to them, mixed liquid foam was then pored on one of the tables and the other was then placed on top and clamped in place to stop it rising to much. Spacers of different sizes were used to achieve the different thicknesses of foam sheets.

These thin sheets were cut into squares 50x50mm, which were subsequently stacked until a similar height to that of the foam blocks was reached. This allows a comparison between the performance of a single block of the foam and a sample of similar dimension made from layers as both have the same energy absorption potential.

Number of Plies	**Area (m^2)**	**Average Ply Thickness (m)**	**Density (Kg/m^3)**
6	0.0025	0.00452	102.0737463
7	0.0025	0.00380	116.8210526
8	0.0025	0.00319	118.3949843
9	0.0025	0.00321	121.9245414

Table 2*, Details of the foamed layer test specimens.*

It can be seen, table 2, that as ply thickness decreases, density increases and that the plies are in the region of two and a half times denser than the blocks, table 2. This can be attributed to the fact that during foaming the plies are constrained to only expand horizontally producing a lot of resistance to expansion whereas the blocks are able to expand vertically. This also means the cells in the foamed layers will be elongated in the horizontal direction and those in the blocks will be elongated vertically, making both specimen types anisotropic.

Uni-axial compression

The above-mentioned specimens were subjected to uni-axial compression tests.

Test parameters:

- Machine used: Zwick/Roell Z250 uni-axial test machine.
- 80 % strain
- Strain rate: 5 mm/min

Figure 1. Foamed layers under compression.

Three phases of deformation are generally observed when compressing polymeric foams. Firstly a linear elastic response is seen, where stress increases linearly with deformation and strain is recoverable. Secondly a stress or collapse plateau, where continued deformation occurs at relatively constant stress. This is where the bulk of the materials energy absorption properties are provided. The final stage is densification; here the material begins to behave like a compacted solid. At this point the cellular structure of the foam has collapsed and further deformation requires the compression of the solid foam material [13]. The collapse plateau starts at the crush strain and ends at the onset strain of densification. [14]

This behaviour was observed in both the foam blocks and layers, although the collapse plateau is clearer in the blocks, Fig 2. There is a large distribution in results, especially in the foam blocks. However the compression lines of the blocks all follow the same shape with collapse strain at around 20% and on set of densification at 68% strain, giving a well defined collapse plateau. The three phases of compression are less pronounced in the foamed layers but still present.

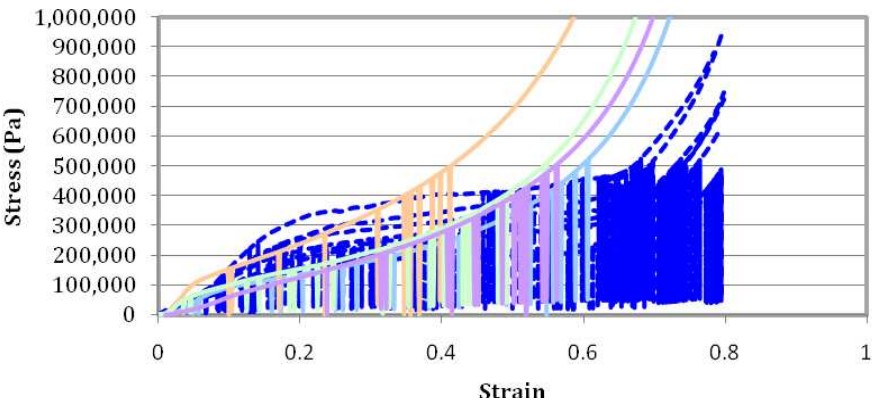

Figure 2. Compressive stress strain graph for PU foam. - - - - PU foam blocks, _____ PU foamed layers.

The distribution in compression stresses can be accounted for by the range of densities of the specimens. Fig 3, showing the stress at 40% strain against the density of each specimen highlights this. For the foam blocks there is a clear linear relationship between compression stress and density, this is not the case for the foamed layers. Forecasting the trend line upwards suggests that foam made in the same way as the blocks but of the density of the layers would absorb more that three times the energy than if it were foamed in layers. From this it could be expected that foam made in blocks will perform better that foamed layers when it comes to the ballistic tests.

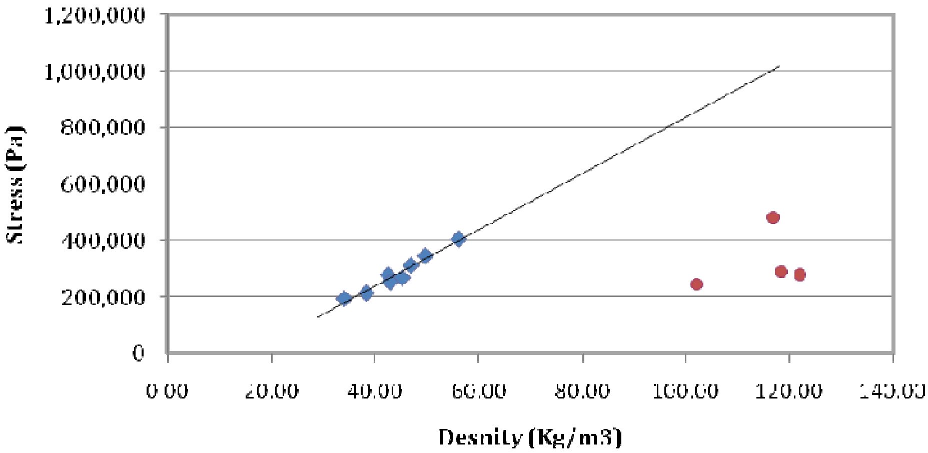

Figure 3. Compressive stress at 40% strain against specimen density, Foam blocks, Foamed Layers.

Looking at the specific properties of the foam we get a clearer picture of it true behaviour, Fig 4. The foam blocks are capable of absorbing much more energy under quasi-static conditions than the foamed sheets.

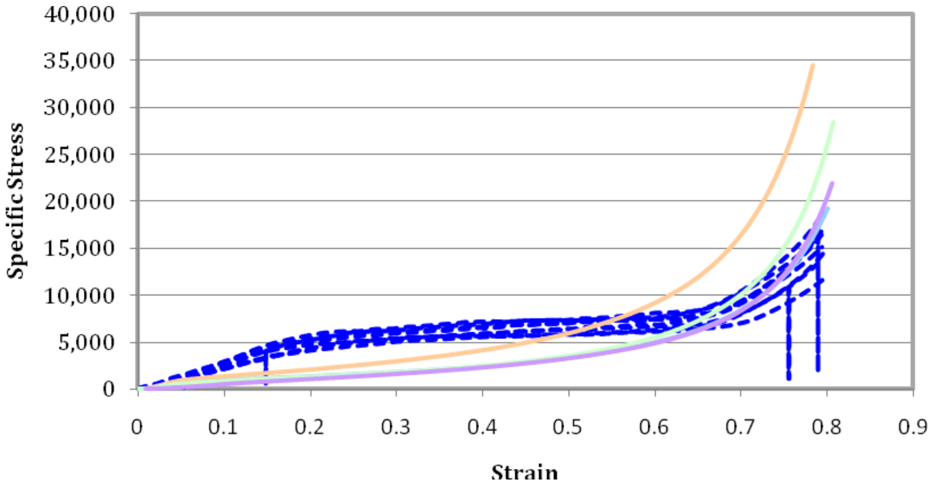

Figure 4. Specific stress strain graph for PU foam. - - - - PU foam blocks, _____ PU foamed layers.

Trauma pack

The aim of a trauma pack is to reduce the depth of the back face signature and the energy transferred from personal body armour to the wearer. Currently some wearers of personal body armour insert steel, ceramic and fabric sections behind the armour in a bid to reduce the BFS. However the insertion of dense, stiff materials such as steel will indeed reduce the depth of BFS to potentially nothing but do little to reduce the energy transfer. The energy from the impact will be spread across the area of the plat reducing the pressure on the torso. The inclusion of materials such as foam will slightly reduce the BFS depth and energy transfer. However as the foam is likely to fracture around the region of impact the energy is not spread over its entire area. The hope is that by utilising the energy absorption properties of foam within a laminar structure both the BFS depth and energy absorbed by the torso can be reduced, incorporating the best of both situations. Foam is also a much lower density that steel and so through its use a much lighter trauma pack could be produced.

Thin layers of foam will be produced and adhered to sheets of an all polypropylene self reinforced composite (srPP); these will then be compiled to form a multi-layer trauma pack. Gilchrist [12] showed that foam impacted at high strain rates, as in ballistic impacts, fractured rather than compressing in the manner expected at lower strain rates. This means the foam dissipates less energy. The idea behind this laminar structure is that the srPP will reduce the likelihood of the foam fracturing in the locality of the impact by distributing the energy over a wider area and so increasing it dynamic energy absorption properties.

It is also hoped that by slicing the foam once it is stuck to the srPP a flexible trauma pack can be achieved. Cutting the foam into much smaller section once it is in place will enable the individual plies to flex easily in one direction and not the other. This should increase the over all trauma pack flexibility without reducing its performance dramatically.

Specimens

The two foaming processes discussed earlier were used to make a range of trauma pack specimens and can be divided in to two categories, those made of layers cut from foam blocks (sliced layers) and those made from layers foamed to specific thicknesses (foamed layers).

Blocks of PU foam were made using a mold with dimensions 200x200x200mm. These blocks were then cut into 25mm and 1.25mm thick sections forming monoliths. Also cut form these blocks were thinner layers to be compiled to the same thickness as the monoliths.

Large sheets of PU foam were produced in varying thicknesses using the same procedure described in the material characterisation section. These sheets were then cut in to squares 190x190 mm. These squares were then stuck to sheets of all srPP of the same size suing Gorilla ™ glue, and complied to form trauma packs of the desired thickness.

Various glues, Loctite ® super glue, Gorilla ™ glue and masking fluid, were tested to see which gave the best adhesion between the PU foam and srPP. It was found the Gorilla ™ glue gave the best hold and so was chosen for the job.

For each set of trauma pack sheet thickness two trauma packs were produced. One of which had the foam sliced in two directions so that the sheets and pack could be bent easily in one direction but not the other. The trauma pack is placed so that it bends in the direction away from the body armor easily but does not bend towards it. This is so that the trauma pack would have some flexibility but not reduce its energy absorption properties dramatically.

Specimens without srPP were also made form the foamed layers to facilitate a fuller comparison. Ideally specimens of sliced layers would also have been made with srPP, however due to the nature of the surface once cut the adhesive would not stick the foam and srPP together.

Details of all the specimens are given in table 3. The ply thicknesses were measured on each side of the specimen and averaged.

	Thickness (m)				Average Thickness (m)	Area (m^2)	Volume (m^3)	Mass (Kg)	Der (Kg
	1	2	3	4					
4 foamed layers, 25mm	0.0063	0.0055	0.0049	0.0058	0.0056	0.0361	0.00020	0.0250	123.
	0.0059	0.0060	0.0059	0.0055	0.0058	0.0357	0.00021	0.0275	132.
	0.0051	0.0058	0.0061	0.0049	0.0055	0.0355	0.00019	0.0260	133.
	0.0055	0.0060	0.0054	0.0058	0.0057	0.0359	0.00020	0.0245	120.
Total Thickness: 0.0226				**Mean**	**0.00565**				**127.**
4 foamed layers, 25mm, flexible	0.0061	0.0058	0.0051	0.0058	0.0057	0.0359	0.00020	0.0270	131.
	0.0061	0.0051	0.0049	0.0050	0.0053	0.0361	0.00019	0.0285	149.
	0.0059	0.0055	0.0058	0.0051	0.0056	0.0355	0.00020	0.0250	126.
	0.0049	0.0055	0.0049	0.0050	0.0051	0.0357	0.00018	0.0250	137.
Total Thickness: 0.0216				**Mean**	**0.00540625**				**136.**
4 foamed layers, flexible	0.00340	0.00346	0.00334	0.00332	0.00338	0.0358	0.00012	0.0185	152.
	0.00298	0.00301	0.00330	0.00350	0.00320	0.0356	0.00011	0.0170	149.
	0.00340	0.00341	0.00314	0.00334	0.00332	0.0362	0.00012	0.0175	145.
	0.00352	0.00384	0.00360	0.00300	0.00349	0.0357	0.00012	0.0165	132.
Total Thickness: 0.0134				**Mean**	**0.0033475**				**144.**
4 foamed layers	0.00374	0.00394	0.00394	0.00354	0.00379	0.0355	0.00013	0.0190	141.
	0.00380	0.00334	0.00330	0.00350	0.00349	0.0360	0.00013	0.0180	143.
	0.00364	0.00350	0.00334	0.00314	0.00341	0.0356	0.00012	0.0180	148.
	0.00394	0.00406	0.00364	0.00398	0.00391	0.0354	0.00014	0.0210	151.
Total Thickness: 0.0140				**Mean**	**0.00364625**				**146.**
3 foamed layers, flexible	0.00422	0.00410	0.00432	0.00450	0.00429	0.0359	0.00015	0.0210	136.
	0.00460	0.00432	0.00450	0.00446	0.00447	0.0342	0.00015	0.0205	133.
	0.00410	0.00432	0.00412	0.00398	0.00413	0.0361	0.00015	0.0210	140.
Total Thickness: 0.0130				**Mean**	**0.004295**				**137.**
3 foamed layers	0.00394	0.00364	0.00422	0.00432	0.00403	0.0359	0.00014	0.0215	148.
	0.00410	0.00390	0.00384	0.00410	0.00399	0.0359	0.00014	0.0195	136.
	0.00458	0.00446	0.00412	0.00412	0.00432	0.0357	0.00015	0.0195	126.
Total Thickness: 0.01294				**Mean**	**0.004111667**				**137.**
2 foamed layers	0.00648	0.00550	0.00608	0.00640	0.00612	0.0353	0.00022	0.0285	132.
	0.00586	0.00550	0.00620	0.00630	0.00597	0.0357	0.00021	0.0270	126.
Total Thickness: 0.01166				**Mean**	**0.00604**				**129.**
13mm monolith (sliced layer)	0.01422	0.01216	0.01254	0.01364	0.01314	0.0372	0.00049	0.0240	49.
25mm monoliths (sliced layers)	0.02670	0.02550	0.02584	0.02564	0.02592	0.0374	0.00097	0.0505	52.
	0.02550	0.02792	0.02874	0.02640	0.02714	0.0369	0.00100	0.0490	48.
	0.02334	0.02050	0.02304	0.02168	0.02214	0.0374	0.00083	0.0425	51.
3 sliced layers	Total Thickness: 0.01776								50.
	Total Thickness: 0.01874								49.
3 sliced layers, no srPP	Total Thickness: 0.01492								111.
	Total Thickness: 0.01632								116.

Table 3. Properties of manufactured trauma packs.

Uni-axial compression

Uni-axial compression tests were performed on sections of the trauma packs with srPP, Fig 5, and it can be seen that the addition of the all srPP and adhesive has no real effect on the compressive behavior compared to the foamed layers alone. It can also be seen that the flexible trauma packs have only slightly reduced compressive strength over there inflexible counterparts.

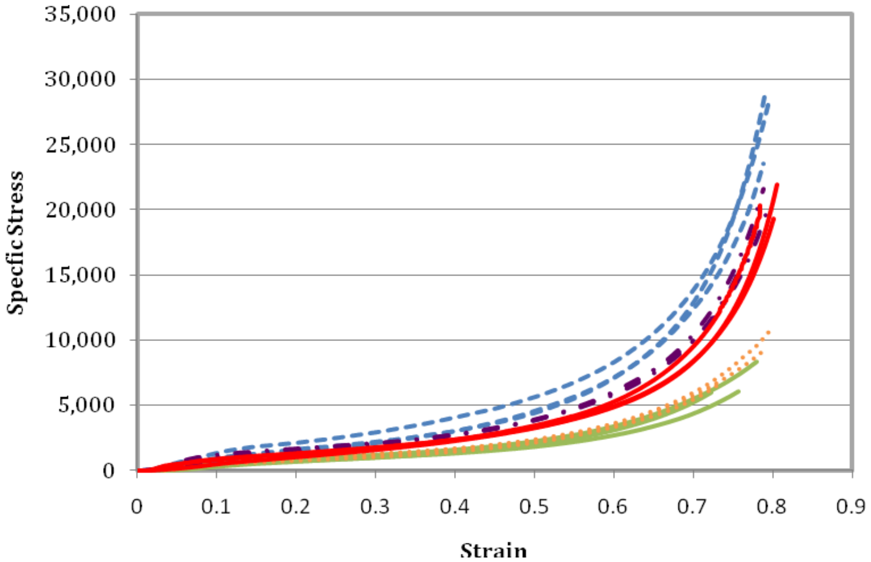

Figure 5, Specific stress strain graph for trauma pack samples. _ _ _ _ _3 foamed layers, _._._._._._.3 foamed layers flexible, _______ foamed layers no srPP,……. 4 foamed layers flexible, ________ 4 foamed layers flexible

Body armor

In order to produce samples of body amour, behind which to test the effectiveness of the trauma pack, sheets of srPP were aligned on top of each other and consolidated in a heat press.

Comment [MSOffice4]: Describe this material – how is it made, what is its structure, who makes it etc

Don & Low Armordom® srPP fabric utilises coextruded polypropylene tapes. Each individual coextruded tape consists of three distinct layers; two lower melting point copolymer PP 'cap' coats on each outer surface encapsulate a higher melting PP core polymer. These tapes are woven into fabric [15]. When heated to or above the melt temperature of the co-polymer coating of the fibers the coating melts and bonds the sheets of fabric together to form a single panel sample.

Where more than one sample with the same consolidation conditions were required multiple sets of sheets were put into the press at the same time separated by sheets of aluminum foil to speed up production. Khan [16] recognized that the temperature indicated on the control dial of the heat press did not correspond to the temperature of the surface of the platens due to its modification and addition of cooling equipment. He devised the below equations to overcome this:

$$\text{Top platen}: y = 1.0217x + 1.4763 \quad (1)$$

$$\text{Bottom platen}: y = 1.0329x + 1.8582 \quad (2)$$

Where x is the temperature on the surface of the platen and y is the set temperature on the control dial.

Comment [MSOffice5]: The temp on the dial should be higher than on the platen – talk to Kyle about this issue, I think Khan made a mistake – should be the inverse I think

Pressure is applied to the press and samples by a hydraulic ram connected to the bottom platen. A gauge on the press gives a read out of the pressure of the hydraulic fluid. In order to find the pressure on the samples Khan [16] established the relationship:

$$\text{Sample presure} = \text{Piston pressure} \times \left(\frac{\text{Piston area}}{\text{Sample area}} \right) \quad (3)$$

Where the piston area is:

$$Piston\ area\ = \frac{\pi D^2}{4} = \frac{\pi \times 0.0187^2}{4} = 0.0187m^2 \qquad (4)$$

Table 4 shows the consolidation conditions of the samples made up, all samples were consolidated for thirty minutes and cooled under pressure.

Number of plies	Sample Pressure MPa	Temperature °C
15	0.16	105
30	0.16	105
30	3.25	165
35	0.16	105

Table 4, Consolidation conditions.

Ballistic testing

In previous work [10] .22 long rifle rounds (0.22 inches in diameter) where fired at specimens of srPP from a single loading target pistol in the interest of assessing the significance of consolidation conditions on the ballistic resistance of srPP. In the interest of consistency the same rifle and type of bullets were used. The samples of body armor and trauma pack specimens were placed in the firing range between a holding plate and the backing material, **** water based modeling clay. . The specimens were constrained to prevent movement other than that caused by deformation due to the projectile, this was achieved by packing the space behind the backing material with catalogs. The back face signature of each specimen was characterised in terms of depth and diameter.

Comment [MSOffice6]: Does this refer to bullet diameter? In mm or inches?

Backing material characterisation

The clay backing material was subjected to uni-axial compression tests to assess its temperature dependency. Tests were performed on specimens at three temperatures; cooled (7°C), room temperature (18°C) and warmed (35°C); and three strain rates; 1,000, 5,000 and 10,000 mm/min. Each test was performed twice. Samples of the clay were made up in block approximately 40x40x36 mm.

Comment [MSOffice7]: Using which machine – name and model

The results, Figs 6, 7 and 8, showed that the clay was indeed temperature dependent but not especially rate dependent. However the temperature dependency was rate dependent. At the higher strain rate the temperature dependency is clearly defined, with the warmer specimens requiring more force for compression. At slower speeds there is still some temperature dependency however it is less well defined.

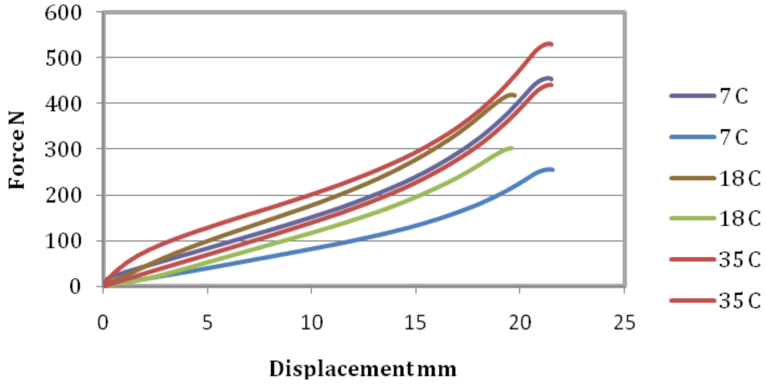

Figure 6, Force/displacement graph of clay backing, strain rate 1000mm/min.

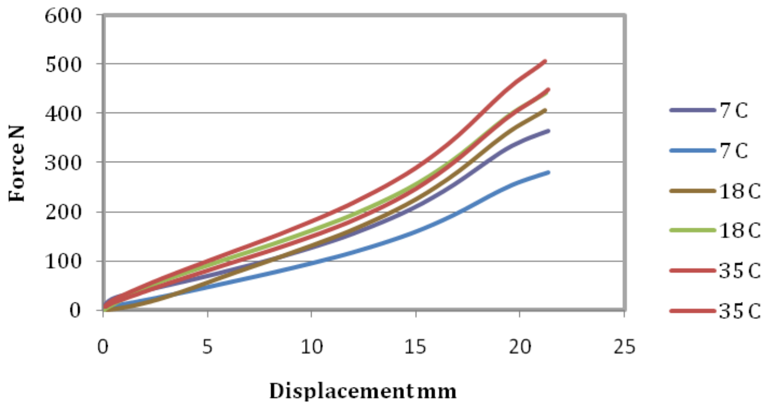

Figure 7, Force/displacement graph of clay backing, strain rate 5000mm/min.

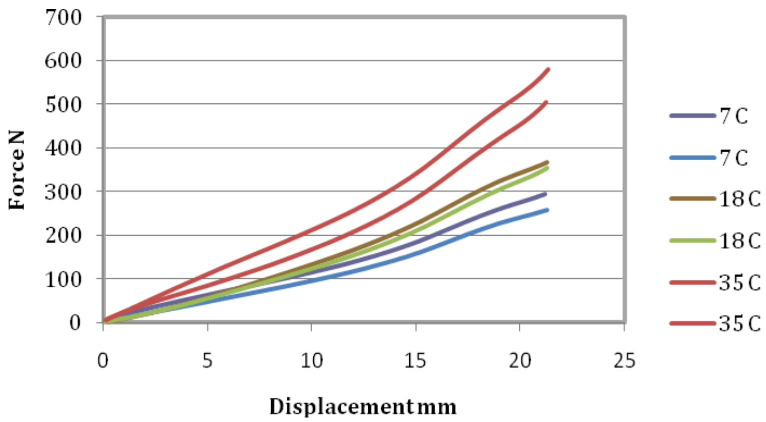

Figure 8, Force/displacement graph of clay backing, strain rate 10,000mm/min.

Calibration drop tests were performed on the backing clay in order to characterise the energy required to deform the clay. After the tests energy per unit volume of deformation was determined in J/m^3. In the tests a bar of mass 1.4 Kg with a spherical end of diameter 52 mm was drop down a hollow tube from heights of 250, 350 and 450mm. As the end of the bar was spherical the trauma shape was taken as a spherical cap. The depth and diameter of each trauma were taken. Using the equation for the volume of a spherical cap:

$$\text{Volume} = 1/6 \times \pi \times h \times (3 \times a^2 + h^2) \tag{6}$$

Where h is the depth of trauma (m) and a is half the trauma diameter (m), the volume of deformation was calculated (m^3). Potential energy of the drop weight was calculated using;

$$EP_{cal} = mgh \tag{7}$$

Where EP_{cal} is the potential energy of the drop weight, m is the drop weighs mass (Kg), g is the gravitational acceleration (ms^{-2}) and h is the drop height (m).

The results from the calibration tests can be seen in figure 9, which clearly shows a linear relationship between energy and deformation volume, with the line equation:

$$y = 225815x + 0.751 \tag{8}$$

Where x is deformation volume and y is the deformation energy. This equation can them be used to calculate the energy transferred to the backing material during the ballistic tests given the BFS volume, to asses trauma pack performance.

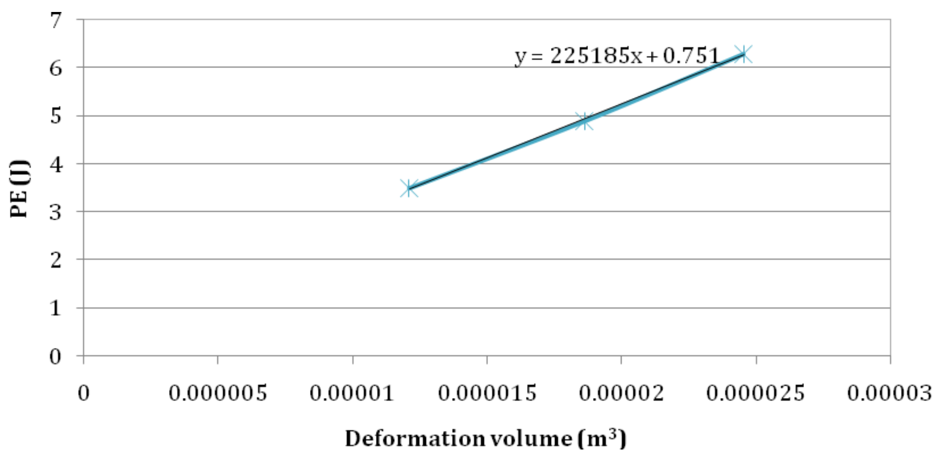

Figure 9, Potential energy / deformation volume graph for drop tests on clay backing.

Body Armor

Milne [10] mounted the specimens on the holding plate in the firing range but it was felt that this might have affected the results so in this work the specimens were not mounted but sandwiched between the holding plate and the backing material.

Comment [MSOffice8]: Was a normal pressure applied to hold the specimen? If so how much? If not say so. What about a photograph?

Table 5 shows a summary of the results from the ballistics tests on the srPP armor. In initial tests the specimens consolidated at 30 ply, 1.62 MPa, 105 °C, successfully stopped the projectile, however in subsequent tests they failed. It was felt that these specimens were at their ballistic limit and so the decision was made to increase the number of plies to 35. The 35 ply specimens never failed and it was these that were used in all-subsequent tests.

Consolidation	Backing material Temperature (°C)	Projectile velocity (m/s)	X diameter (mm)	Y diameter (mm)	BFS Depth (mm)
15 ply, 0.16 MPa, 105 °C	19.8	327	**Did not stop projectile**		
30 ply, 0.16 MPa, 105 °C	20.2	311	**Did not stop projectile**		
30 ply, 1.62 MPa, 105 °C	20.0	328	55	60	25.00
	19.6	328	55	55	25.20
	19.7	318	50	50	25.28
30 ply, 3.25 MPa, 105 °C	20	317	**Did not stop projectile**		
35 ply, 1.62 MPa, 105 °C	19.7	312	44.5	47.2	22.59
	20.4	322	44.9	46.5	23.48
	19.5	318	47.6	45	24.05

Table 5, Ballistic tests results of srPP body armor.

Trauma Packs

Several problems were encountered when analysing the results. Because of the two foaming processes used, as discussed earlier there are two sets of densities, low for the sliced layers and high for the foamed layers. Also because trauma pack thickness is to be investigated different numbers of layers and ply thicknesses were used.

The results will be looked at from two view points, optimisation from mass, taking into account the foam density, and optimisation for thickness.

Looking at the BFS depth against trauma pack thickness, Fig 10, shows that as would be expected placing foam behind the armor reduces the BFS depth. However there is a clear distinction between those trauma packs with the laminate structure of PU foam stuck to sheets of all srPP and those without, those without srPP clearly performing worse. Looking only at BFS depth seems to show that there is little difference in the performance between the two foaming processes, the foamed layers with out srPP were no better that the sliced layers also without srPP.

The number of plies used to make up the trauma pack also has negligible effect on its performance with the three packs made from foamed layers of 2, 3 and 4 plies all resulting in similar trauma depths, figure 12.

Dividing the DFS depth by the individual foam densities, fig 13, gives a much clearer indication of the performance difference between the different trauma pack structures. The foamed layers with srPP perform about five times better than the sliced layers and twice as well as the foamed layers without srPP.

◆	srPP armor
■	Sliced layer monolith
+	3 ply, foamed layers, no srPP
●	3 ply, sliced layer
▲	2 ply, foamed layers
X	3 ply, foamed layers
X	4 ply, foamed layers

Table 6, Ballistics graphs key.

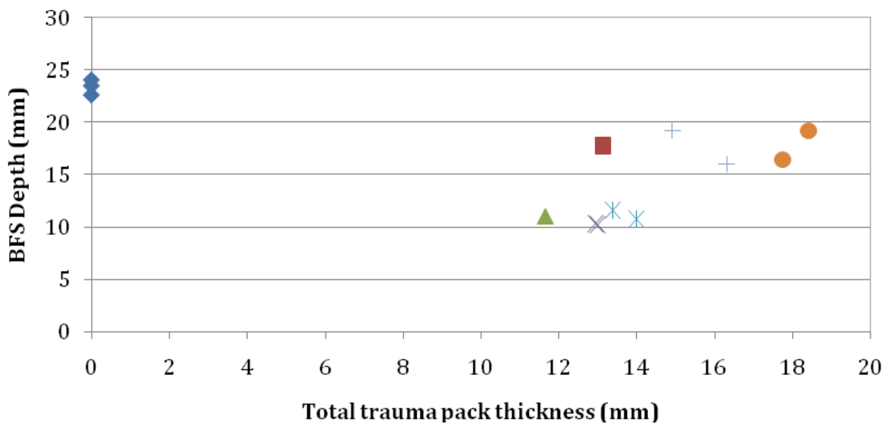

Figure 10, BFS depth / total trauma pack thickness for manufactured trauma packs.

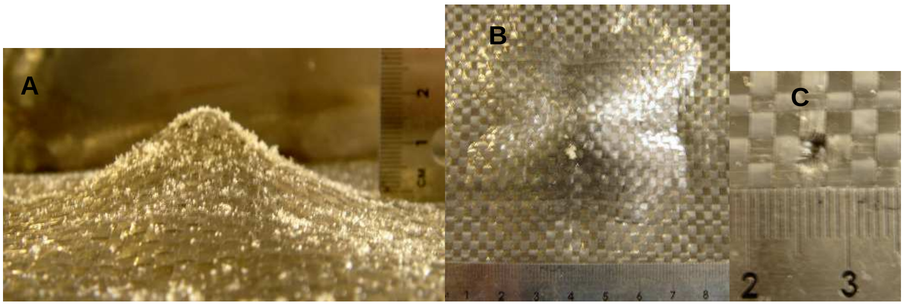

Figure 11, srPP armor after ballistic test. A) BFS side view, B) BFS top view, C) Entry hole on impact face.

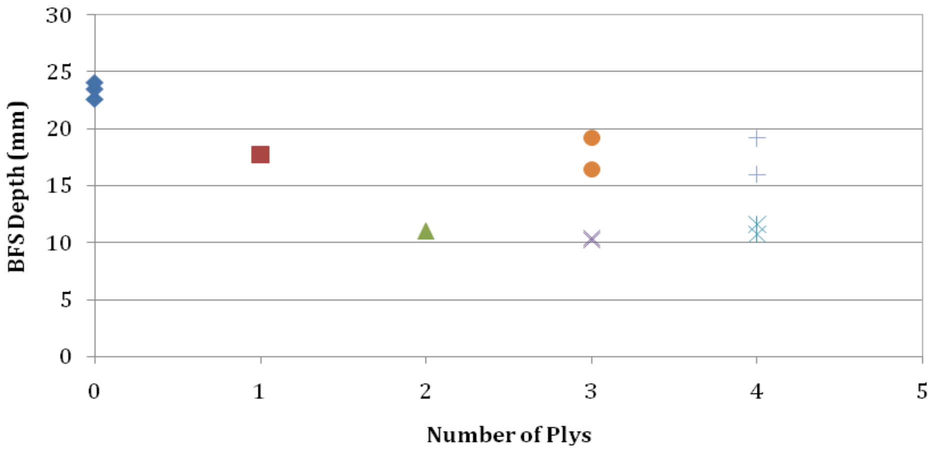

Figure 12, BFS Depth / Number of Plies, for manufactured trauma packs.

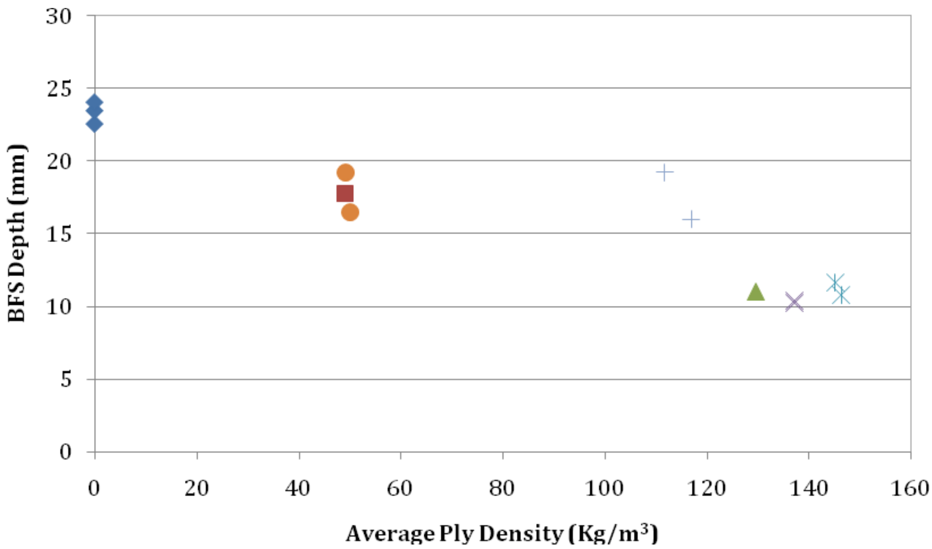

Figure 13, BFS depth / average ply density of trauma packs.

Molds of some of the BFSs were taken, Fig 15, in order to properly characterise the geometry of the clay deformation. Measurements were taken at 5mm intervals and at points of large diameter change, these were then plotted on graphs alongside the arc of a circle centered on the y-axis. The circles arc was plotted by saying the DFS diameter and depth are the cord length and segment height of the circle respectfully. The equation of a circle is:

$$(x+a)^2+(y+b)^2=r^2 \tag{9}$$

this can be rearranged to give y:

$$y=\sqrt{r^2-(x+a)^2}-b \tag{10}$$

a = 0, as the circle is centered on the *y* axis, *r* and b can be found from circle geometry.

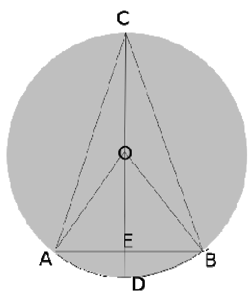

AB = cord length = BFS diameter.

ED = segment height = BFS depth.

AO= radius, *r*

$$CE=\frac{AB^2}{4ED} \tag{11}$$

$$Radius,\ AO=\frac{(CE+ED)}{4} \tag{12}$$

$$b=-(r-ED) \tag{13}$$

The circle arc was then plotted between 0, the circle centerline and the radius of deformation (half the cord length). It can be seen that the area under the curves is reasonable similar. This demonstrates that approximating the volume of deformation to that of a spherical cap will give a fair representation of the actual volume.

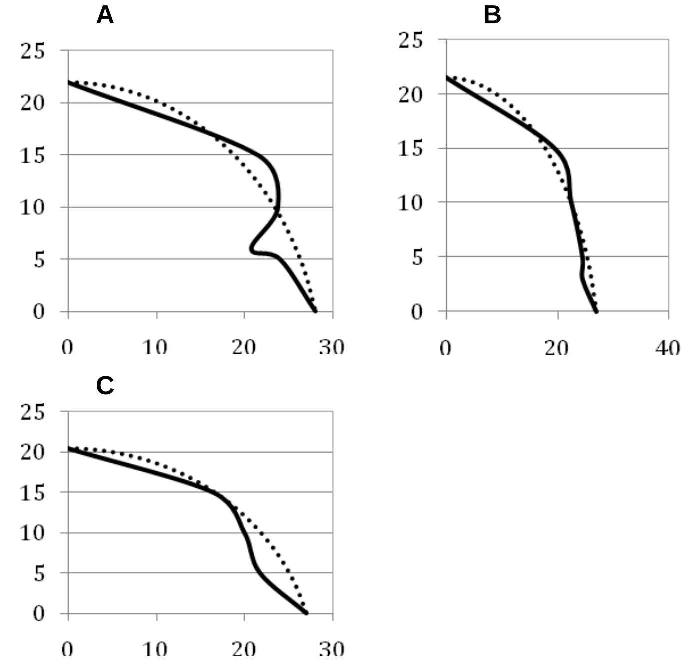

Figure 14, Graphed geometries of BFS molds, _______ BFS geometry, …….. Spherical cap.

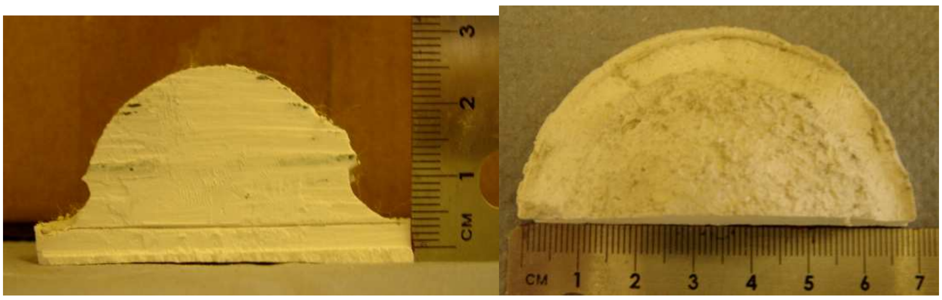

Figure 15, BFS molds made form plaster.

Having established the BFS volume can be approximated to that of a spherical cap the volumes of deformation were calculated to enable the calculation of the energy transferred to the clay backing, sing equation 8, y = 225815x + 0.751, where x is the volume of deformation and y is the energy transferred to the clay. Fig 16. This graph shows that the sliced layer monolith performed best, transferring the least energy, and the foamed layers performed worst transferring the most out of all the trauma packs. However dividing the energy transfer by the density and plotting this against trauma pack thickness shows that the foamed layers with srPP is actually the best performer, Fig 17. On this graph the ideal trauma pack would be placed in the bottom left hand corner, near the origin. This would mean that for a specific density of foam the pack would transfer very little energy and still be very thin. The foamed layers with srPP are the nearest to this. The lines A, B, and C are the trend lines for the three types of trauma pack, sliced layers, foamed layers with no srPP and foamed layers with srPP respectively. A trauma pack made from sliced layers would need to be around 34mm thick to completely stop the energy transfer, one comprising foamed layers with no srPP 25mm and the foamed layers with srPP, only 17mm thick.

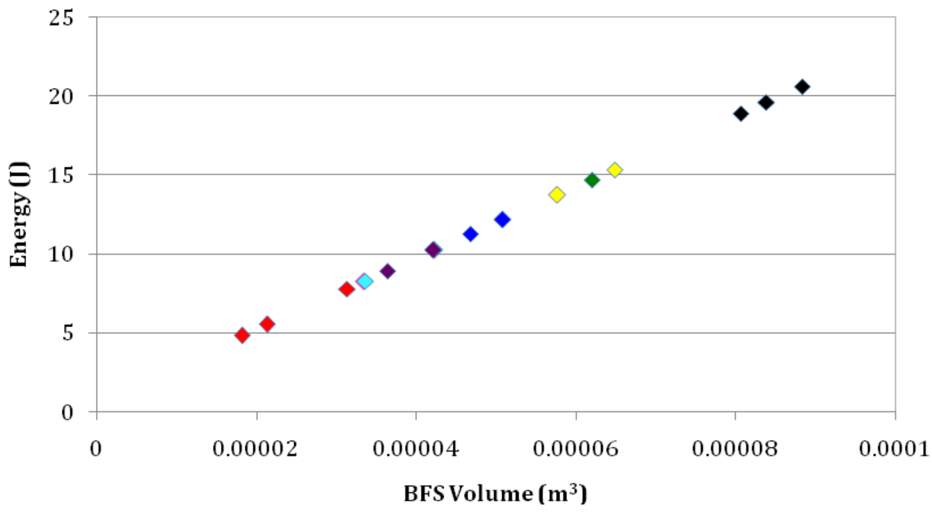

Figure 16, Deformation energy / BFS volume for trauma packs.

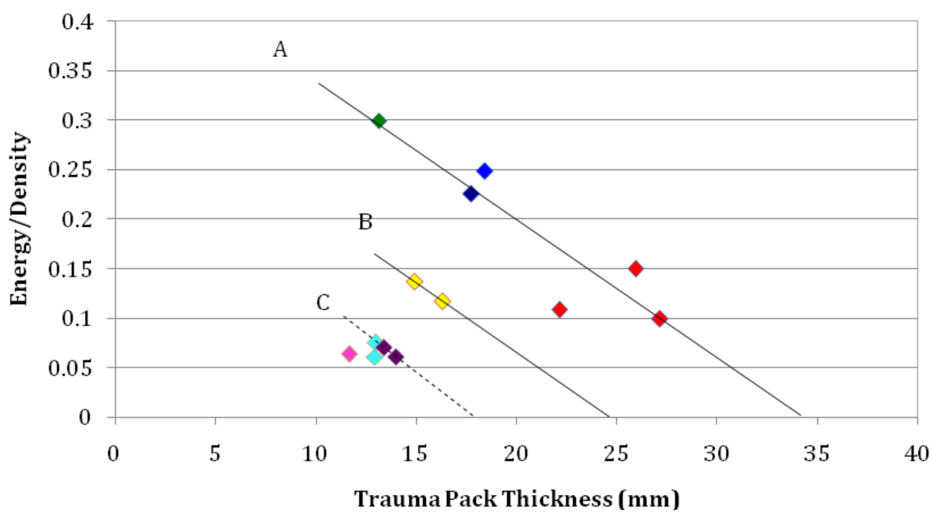

Figure 17, Energy/trauma pack density / trauma pack thickness.

Figure 18, shows the impact face between the armor and trauma pack of four of the trauma packs. There is a clear difference in deformation between the foamed (A, B, C) and sliced (D) layers, the foamed layers fracture around the impact zone, the red lines showing fracture lines. The sliced layer however has no fracture lines and the foam in the impact zone appeared to disintegrate, this would suggest contrary to the results the sliced layers would have absorbed more energy. There is also a difference in response between the trauma packs with srPP and those without; B and D have a hole in the center of deformation. It can be seen that in A and C, those with srPP the diameter of the fracture zone is approximately 4cm where as in B, the foamed layers with no srPP it is approximately 5cm. This suggests the srPP has not helped to spread the energy of impact over a larger area. However looking at Figure 19 A and 19 B, we see the progression of deformation through the plies of a trauma pack with (B) and without (A) srPP. In A, serious fracture occurs in each layer of the trauma pack where as in B, the amount of fracturing greatly decreases through the plies. This implies that although the fracture zone is smaller on the impact face of the trauma pack with srPP compared to without, the srPP is spreading the energy for the layer of foam behind it. This would explain why the trauma packs with srPP reduce the energy transferred to the backing material more than those without.

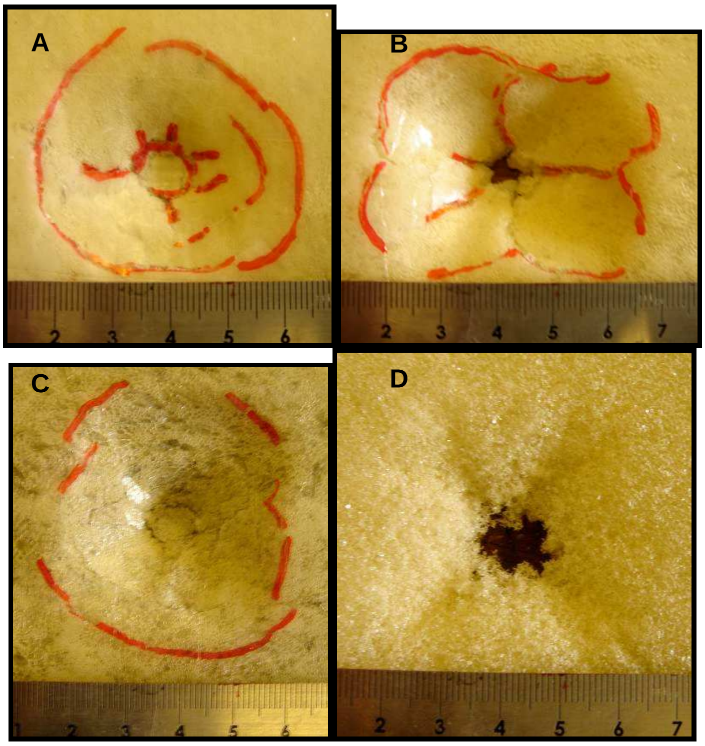

Figure 18, The impact face of four trauma packs. A) 3 ply foamed layers with srPP. B) 3 ply foamed layers with no srPP. C) 4 ply foamed layers with srPP. D) 3 ply sliced layers no srPP.

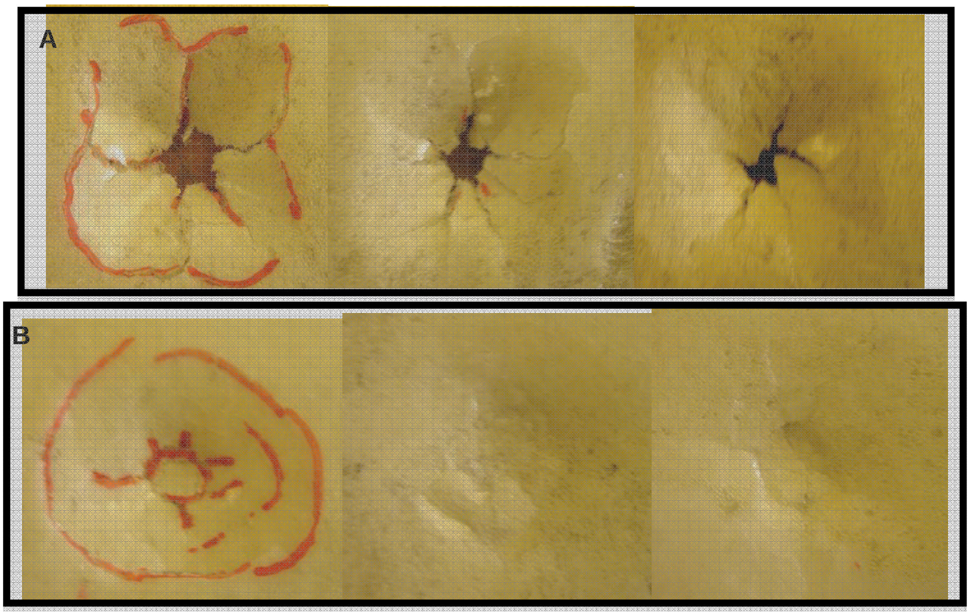

Figure 19, The progression of deformation through two trauma packs, A) Foamed layers without srPP, B) Foamed layers with srPP.

Discussion

Future Work

References

[1] International Journal of Impact Engineering 30 (2004) 665–683, Finite element study of high-speed blunt impact on thorax: linear elastic considerations, Quentin Grimal, Bazle A. Gama, Salah Naili, Alexandre Watzky, John W. Gillespie Jr.

[2] Wilhelm M, Bir C. Injuries to law enforcement officers: The back face signature injury. Forensic Science International 174 (2008) 6–11

[3] National Institue of Justice. Ballistic resistance of personal body armour, NIJ Standard 0101.06.

[4] Gryth, D. 2007, Severe Lung Contusion and Death after High-Velocity Behind-Armor Blunt Trauma: Relation to Protection Level, MILITARY MEDICINE, 172, 10; 1110.

[5] Drobin D, Gryth D, Persson J K E, Rockse´ n D, Arborelius U P, Olsson L, Bursell J, and Kjellstro¨ m B. Electroencephalogram, Circulation, and Lung Function After High-Velocity Behind Armor Blunt Trauma. The Journal of TRAUMA Injury, Infection, and Critical Care. Volume 63 number 2, pp 405-413.

[6] Roberts J C, Ward E E, Merkle A C, and O'Connor J V. Assessing Behind Armor Blunt Trauma in Accordance With the National Institute of Justice Standard for Personal Body Armor Protection Using Finite Element Modeling. The Journal of TRAUMA Injury, Infection, and Critical Care. Volume 62, number 5, pp 1127-1133.

[7] Sriram R, 2006, Blast impact response of aluminum foam composites, J MATER SCI 41, 4 0 2 3 –4 0 3 9

[8] Brown R, 1999, Hand book of polymer testing: physical methods, CRC Press.

[9] Ellis RL, Ballistic impact resistance of Graphite Epoxy composits with shape memory alloy and extended chain Polyethylene Spectra TM hybrid components, Unpublished MSc project, 1996 - Virginia Polytechnuc Institute and State University.

[10] Milne S. Static and Dynamic Mechanical Testing of an all Polypropylene Self-Reinforced Composite (Armordon). Unpublished BEng Project 2008 – University of Glasgow.

[11] Shim V, Yap K (1997). Static and Impact Crushing of Layered Foam-Plate Systems. *Int. J. Mech S¢i* VoL 39, No. 1, pp. 69-86.

[12] Gilchrist A, Mills, N J. (2001), Impact deformation of rigid polymeric foams: experiments and FEA modeling. International Journal of Impact Engineering 25 (2001) 767–786.

[13] Ouellet S, Cronin D, Worswick M. Compressive response of polymeric foams under quasi-static, medium and high strain rate conditions. Polymer Testing 25 (2006) 731–743.

[14] Magkiriadis Q. M. Li, I. and Harrigan J. J. (2006) Compressive Strain at the Onset of Densification of Cellular Solids. *Journal of Cellular Plastics*; 42; 371.

[15] Don & Low Armordon Self Reinforcing Polypropylene (srPP) Product Guide.

[16] Khan M. Consolidation of Self-Reinforced Composites and Testing of Mechanical Properties, Unpublished MSc Project, 2007 – University of Glasgow.

Comment [MSOffice9]: NAMES SHOULD BE BEFORE TITLE

Comment [MSOffice10]: Use same format for each reference

Comment [MSOffice11]: Year?

Deleted: e

Deleted: .

Comment [MSOffice12]: Year cited 2x

Appendix